Study of hygroscopic stresses in asymmetric biocomposite laminates

Mael Péron, Amandine Célino, Mickael Castro, Frédéric Jacquemin, Antoine Le Duigou

Study of hygroscopic stresses in asymmetric biocomposite laminates

Mael Péron[1], Amandine Célino[1], Mickael Castro[2], Frédéric Jacquemin[1] and Antoine Le Duigou[2]

1: Université de Nantes
GeM, Institut de Recherche en Génie Civil et Mécanique, Equipe E3M
58 rue Michel Ange, BP420, 44600 Saint-Nazaire - France

2: Univ Bretagne-Sud
IRDL UMR CNRS 6027, Pole Thématique Composite,
Rue Saint-Maudé, B 92 116, 56321 Lorient Cedex - France

*Corresponding author: antoine.le-duigou@univ-ubs.fr

Abstract

The hygro-mechanical behaviour of a bio-sourced composite material (MAPP/flax) is experimentally investigated through the characterization of its moisture diffusion and elastic properties, as well as the in-plane hygroscopic swelling of a unidirectional ply sequence and curvature in the case of an asymmetric lay-up sequence. From these considerations, we propose a hygro-mechanical model for the material behaviour, based on a Fickian diffusion model solved in 1D with a finite difference method, and coupled to a modified mechanical model based on laminate theory. The proposed model takes into account the evolution of the mechanical properties as well as hygroscopic swelling during moisture uptake to predict the stress state during water sorption of a biocomposite. Results show that sorption kinetics is dependent on the lay-up sequence of the biocomposite structure. The stress state determined from the thickness of the asymmetric lay-up shows that most of the plies (approx. 75% of the whole laminate) are subjected to a compressive stress along their in-plane direction transverse to the fibres. This stress distribution may lead to a decrease in the free-volume of the material, thus modifying the hygroscopic properties by reducing its maximum moisture content compared to the unidirectional laminate (the stress distribution being equal to zero for this latter laminate when saturation is reached).

Keywords: natural fibre, moisture, hygroscopic stress, asymmetrical laminate

1. Introduction

Natural fibres such as flax have a strongly hydrophilic behaviour that leads to a high level of moisture absorption, around 20-25% at 95% RH [1], combined with a large anisotropic swelling deformation. The degree of hygroscopic deformation is higher in natural fibres compared with synthetic fibres (glass or carbon), and therefore requires careful attention for biocomposite design.

Indeed, transverse hygroscopic expansion of a single flax fibre reaches 21 ± 3 % at 95% RH [2]. This hygroscopic strain is linked to the fibre microstructure (*i.e.* microfibril angle and biochemical composition) and explains, for example, why coir fibres swell less than flax fibres [3]. Assuming circular cross-section, the coefficient of hygroscopic expansion of a single flax fibre in the transverse

direction β_{fT}, as determined in the range 20-95% RH, attains 0.0114 $\varepsilon/\%_{moist.\ content}$ [2], which is drastically higher than its Coefficient of Thermal Expansion (CTE) α_{fT} (78.10^{-6}/°C)[4].

At the scale of the ply and laminate, the change in humidity induces an overall change of the natural fibre reinforced composites sample geometry as a function of the fibre orientation, content, microfibril angle and biochemical composition [5]. The surrounding matrix produces a constraining effect on flax fibres that reduces the fibre-free hygroexpansion and leads to a compressive state which promotes load transfer within biocomposites [2][6]. The constraining effect of the matrix also causes a reduction of the fibre's accessibility to water [7][8].

However, the difference of swelling strain at the fibre/matrix interface is often cited as a major source of damage that reduces biocomposite lifetime [9]. Indeed, numerous reviews in the literature claim that differential swelling between a natural fibre and a polymer leads to matrix cracking, interface debonding and ply delamination [9][10] [11].

This mechanism and the stress state generated within biocomposites have been only rarely studied in the literature. Consequently, this aspect should be addressed to ensure the durability of biocomposite parts.

Experimental techniques to estimate residual stresses have been reviewed by Parlevliet *et al.* [12]. Among these techniques, asymmetrical laminates subjected to environmental variations provide a simple but indirect indication of residual stresses through the measurement of out-of-plane deformation. Such laminates based on synthetic materials have been used, for example, to reveal curing [13] or hygrothermal stresses [14]. Recently, asymmetric biocomposite laminates have been used to develop bioinspired hygromorph composites with an original actuation functionality, *i.e.* a large out-of-plane displacement or curvature triggered by a moisture gradient [3][5][15][16][17]. In these cases, actuation is mainly due to hygroscopic radial stresses around natural fibres.

Once the hygroscopic behaviour and properties of the material have been experimentally determined, it is possible to model its behaviour under environmental conditions, and hence the associated residual stresses. More complete approaches based on both experimental and numerical investigations have been performed using petro-based materials [7,18–24]. Two main approaches stem from the literature.

The first approach, called *uncoupled* modelling, only takes into account the impact of moisture uptake on hygroscopic swelling and associated stresses [19–21,23,24]. Uncoupled modelling as applied in many studies allows a satisfactory reproduction of moisture uptake. However, it often fails to account for plasticization, or the impact of stress intensity on the hygroscopic behaviour. The predicted internal stresses may therefore be overestimated. Although *coupled* modelling is based on uncoupled modelling, it also considers the impact of the stress state on the moisture diffusion process, as well as on the mechanical properties of the composite [7,18,22]. This more comprehensive modeling approach allows an accurate reproduction of the material behaviour, but requires a versatile characterization of the material to identify the multiple phenomena involved. These multi-physical models, whether uncoupled or coupled, are only rarely applied to the study of bio-sourced materials [25]. Therefore, research along these lines would allow a better understanding of natural fibre based composites submitted to variable environmental loadings.

In this context, the aim of our study is to gain a deeper insight into hygroscopic swelling and the consequent stress state occurring in natural fibre composites exposed to hygrothermal variations. In the present study, we use $[0/90\ ]_{ns}$ non-symmetrical laminates of maleic anhydride grafted polypropylene (MAPP)/flax composites subjected to water immersion. In this way, we can evaluate, both experimentally and numerically, the strain and stress states within the material as well as the coupling between diffusion and swelling. At the ply scale, experimental procedures are applied here to measure the diffusion kinetics, the anisotropic hygroscopic dilatation and mechanical properties of a unidirectional MAPP/flax biocomposite. Then, we investigate the response of an asymmetric MAPP/flax $[0_1/90_5]$ lay-up to hygroscopic loading at the laminate scale by measuring its curvature during moisture sorption. Finally, we make use of a multiphysical model built from the modified laminate theory to identify the sorption kinetics, the distribution of moisture content as well as the strain and stress states across the sample due to gradients in moisture content during sorption.

2. Materials and methods

2.1. Materials

Flax fibres (*Linum usitatissimum*) were harvested in France and then dew retted before being scutched and hackled. Unidirectional flax fibre tapes (50 g/m²) were supplied by Lineo®. The polymer films were made up of film-casted polypropylene (PP) (PPC 3660 from Total Petrochemicals) and compatibilized PP with 4% PP grafted maleic anhydride (MAPP) (Arkema Orevac CA 100). Then, a stack of polymer films (PP + MAPP) and unidirectional flax-fibre tapes were prepared in a metallic mould (130 x 130 mm²). Composite laminates were manufactured with a dedicated hot pressing protocol, heated at 190°C for 8 min at a pressure of 20 bars with an incremental pressure application to maintain the fibre alignment [26]. The cooling ramp was set to 15°C/min. The flax fibre content was set at 60 % by volume. Two different lay-ups were manufactured, one unidirectional [90_6] and the other asymmetric [0_1,90_5]. This latter configuration is based on a stacking that produces an optimal curvature response when subjected to moisture absorption [3][17]. The overall thickness was 0.46 ± 0.02 mm and the porosity volume fraction was Vp = 1.35± 0.20%. Strips of 70 mm x 10 mm were machine-milled for the curvature measurements. A high length-to-width ratio was chosen to reduce the risk of double curvature [27]. The materials were then stored under equilibrium conditions (T= 23°C and RH= 50%) until the weight reached a constant value.

2.2. Experimental methods

2.2.1. Diffusion

Unidirectional and asymmetric biocomposites were stored at 50% RH and 23°C to allow attainment of a reference state. Then, the materials were immersed in deionized water at room temperature. During immersion, the samples were periodically removed to be weighed (using a balance with an accuracy of 10^{-4} g) and characterized. The percentage gain C_{mean} at time t is calculated as:

$$C_{mean}(t) = \frac{W_t - W_o}{W_0}.100 \qquad \text{(Equation 1)}$$

where W_t and W_0 are the weight of sample at time t after water exposure and the weight of the dry material before immersion (for RH=50% and T=23°C), respectively. The maximum moisture absorption C_s is calculated as the average value of five consecutive measurements where each measurement has been performed on 5 samples and averaged arithmetically.

2.2.2. Hygroscopic dilatation

Transverse and longitudinal dilatation due to moisture sorption (hygroscopic dilatation) were periodically measured with a micrometer (with an accuracy of ± 1 µm) on unidirectional biocomposites during the sorption phase. Three square biocomposite samples of 20 mm X 20 mm were cut out. Then, three lines were traced longitudinally and transversally to the fibre direction to ensure that the swelling measurements were always performed at the same point. The results were then averaged arithmetically.

2.2.3. Hygro-elastic properties

The tensile properties of dry and wet unidirectional biocomposites with flax fibre orientation set at 0° (E_L) and 90° (E_T) were measured separately according to ISO 527-4 standards, using an Instron 5566 universal testing machine (cell load 10 kN) at controlled temperature (23°C) with a crosshead speed of 1 mm/min. The samples have the following dimensions (thickness t and width w): $t_{0°}$ = 1 mm and width $w_{0°}$ = 15 mm; $t_{90°}$= 2 mm and $w_{90°}$=25 mm. Mechanical tests were performed on samples that had reached their saturation time. An axial extensometer with a nominal length of 25 mm (L_0) was used to measure the strain. Tensile modulus is determined within a range of strains between 0.05 and 0.1 % according to the procedure suggested by Shah et al [28].

2.2.4. Curvature

The bending curvature of the asymmetric biocomposites $[0_1,90_5]$ during immersion in deionized water was estimated by periodically taking images of one side of the clamped sample ($L_{clamped}\approx$ 10 mm). Image analysis was performed using ImageJ® software (National Institutes of Health, USA). The curvature was measured by fitting the time-evolution of the sample to a 'circle' function. Bending curvature (K) was calculated with the radius of the fitted circle. More information can be found in [17].

3. Experimental results

3.1. Diffusion kinetics

Figure 1 presents the diffusion kinetics obtained by gravimetric measurements on unidirectional $[90_6]$ and asymmetric MAPP/flax composite $[0_1, 90_5]$ laminates, as a function of the square root of time *t*. For both materials, the diffusion behaviour is characterized by two distinct sections: a linear part is

visible on the left of the graph, followed by a saturation plateau that corresponds to the maximal moisture absorption C_s. This behaviour is typical of a Fickian diffusion process, which is then used as a first approach to describe the diffusion kinetics.

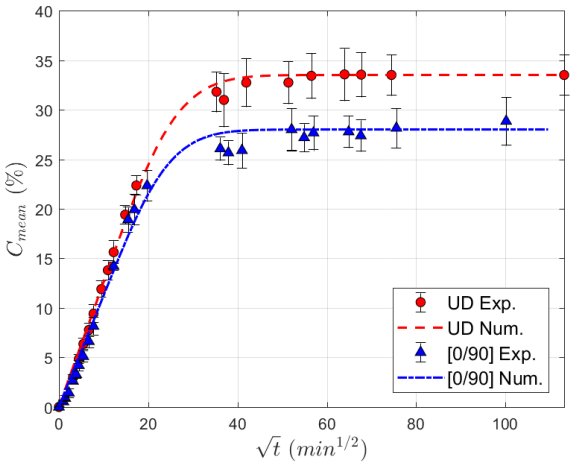

Figure. 1. Diffusion kinetics of unidirectional [0_6] and asymmetrical [0_1 ,90_5] biocomposite laminates. The dashed curves represent the evolution of numerical mean moisture content C_{mean} given by the Fick model

In the present case, geometrical considerations lead us to assume a one-dimensional diffusion due to the very small thickness of the laminates (e = 0.46 ± 0.02 mm) compared to their in-plane dimensions. An analytical solution is given by Crank [29] for thin plates, which provides a constant diffusion coefficient (Eq.2).

$$C_{mean}(t) = \left(1 - \frac{8}{\pi^2}\sum_{n=0}^{\infty}\frac{1}{(2n+1)^2}\exp\left(D\left(\frac{2n+1}{e}\right)^2\pi^2 t\right)\right) \times C_s, \qquad \text{(Equation. 2)}$$

where C_s is the saturation moisture content (%) and D corresponds to the diffusion coefficient (mm²/s).

The diffusion coefficients of unidirectional biocomposites and asymmetric laminates are calculated from this equation and experimental data by minimizing the quadratic sum of the difference between experimental and predicted values. Numerical results are computed using the open source software *Scilab*© and are also presented in figure 1, showing a good agreement with the experimental data which allows us to validate the model used here. The determined diffusion coefficients and saturation moisture contents for both ply sequences are summarized in Table 1.

	D (mm²/s)	**Cs (%)**
Unidirectional [90_6]	$1.07.10^{-6}$	33
Asymmetrical [0_1, 90_5]	$0.96.10^{-6}$	28

Table 1 Identification of diffusion parameters according to the Fick model

The type of laminate lay-up does not lead to any significant change of the diffusion coefficient. The values obtained for Fickian diffusion are in the same range as those published elsewhere on natural fibre composites [30]. However, we note a clear dependence of the maximal moisture sorption on the ply sequence (Figure 1). The mechanical state resulting from the asymmetrical lay-up influences the moisture sorption capacity of the biocomposite.

This mechanical state corresponding to the asymmetric MAPP/flax biocomposite is calculated and further discussed in Section 5.

3.2. Hygroscopic expansion

Figure 2 shows the evolution of relative transversal and longitudinal hygroscopic strain (ε^{hygr}) of a unidirectional [90_6] biocomposite as a function of the mean moisture content C_{mean} . A well-marked anisotropic behaviour is observed when longitudinal swelling is close to zero, while transverse swelling reaches a maximum relative displacement of 3.20 ± 0.17 %. Under similar environmental conditions, a single flax fibre exhibits a transverse strain of 21 ± 3 % at 95% RH [2]. Therefore, a constraining effect of the matrix on the flax fibres is observed at the ply scale, which confirms the results obtained by Joffre *et al* [8].

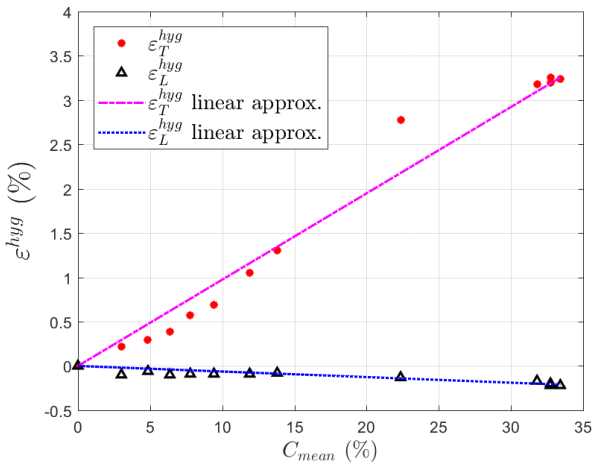

Figure 2: Evolution of longitudinal and transverse hygroscopic strains. Red and black dots represent experimental data and continuous lines represent theoretical results from model.

As an initial approximation, the hygroscopic strains ε^{hyg} along the longitudinal and transverse directions, respectively, denoted with the subscripts L and T, are assumed to evolve linearly with moisture content C_{mean}:

$$\varepsilon_i^{hyg} = \beta_i \Delta C_{mean} \qquad \text{(Equation 3)}$$

where $i = L$ or T, β_i is the hygroscopic swelling coefficient for direction i and ΔC_{mean} is the difference of moisture content between the current state and the initial state of the material. Therefore, β_i is constant over the whole range of moisture uptake and can be obtained by dividing the hygroscopic strain at saturation ε_i^{hyg} ($t = t_{saturation}$) by the final moisture content C_s. The obtained coefficients of moisture expansion are β_L = -6.29 10^{-5} and β_T = 9.74 10^{-4} ε/%$_{\text{moist. content}}$. The theoretical strains obtained from these coefficients are represented in Figure 2, showing a good agreement with experimental data.

3.3. Hygroelastic properties

Figure 3 presents the hygro-elastic properties of the composite (i.e. longitudinal and transverse Young's moduli E, strain ε and strength at break σ) determined by tensile tests.

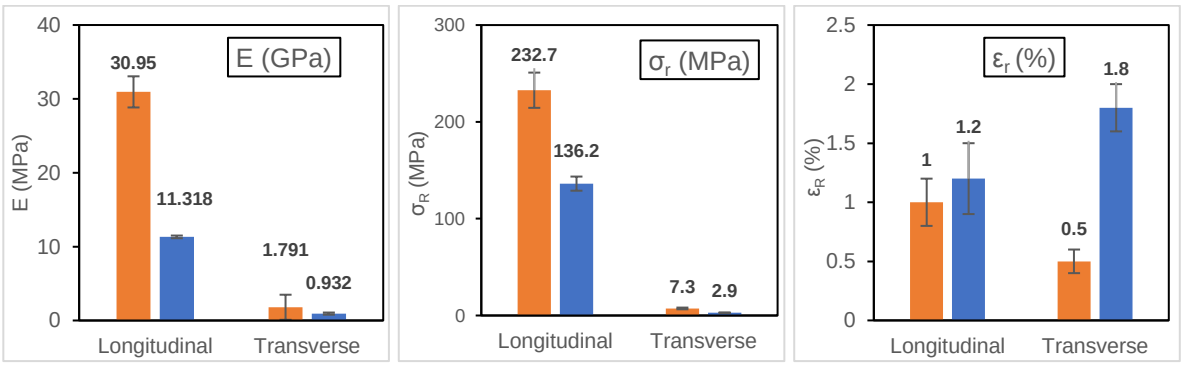

Figure 3. Longitudinal and transverse hygro-elastic mechanical properties at break of dry and wet unidirectional biocomposites: Tensile Modulus E, Stress at break (σ_r) and strain at break (ε_r) (orange for dry state and blue for wet state)

We observe a clear effect of plasticization on the mechanical properties due to moisture uptake, which leads to a large decrease of the tensile moduli and strength at break associated with an increase of elongation in both directions. A full understanding of the variation of the longitudinal and transverse

Tensile moduli with moisture content is necessary to predict the material behaviour during moisture sorption. In the present study, the tensile modulus is assumed to show a large decrease at low moisture contents (C_{mean} < 5%). This type of evolution has already been demonstrated in the literature [31] and is shown in figure 4.

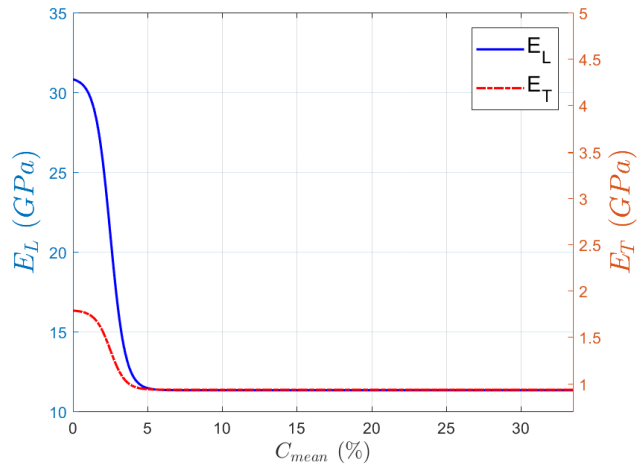

Figure. 4. Evolution of transverse and longitudinal Young's moduli as a function of water content C_{mean}.

3.4 Curvature evaluation

During the sorption step (Figure 5), the curvature of the asymmetric laminate shows a quasi-linear variation with water content C_{mean} up to 5-7 %. At higher values, a break in the slope is observed which corresponds to a stabilization of curvature with increasing water uptake.

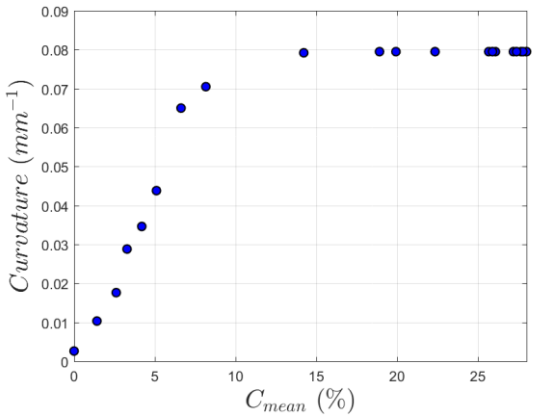

Figure. 5. Evolution of laminate curvature as a function of water content C_{mean}.

4. Numerical modelling

A hygro-mechanical model is developed here to reproduce the hygroscopic behaviour of the composite material and the evolution of its curvature during immersion. This model considers a weak coupling

between water diffusion and the mechanical behaviour of the material. Although water uptake induces hygroscopic swelling and a deterioration in the mechanical properties of the composite (plasticization), the stress state does not modify the moisture diffusion coefficient (D and Cs). The diffusion problem is solved first, allowing us to determine the water content distribution in the laminate. Then, the mechanical problem is solved by taking into account the hygroscopic swelling and the plasticization due to the previously calculated water contents. In the following sub-sections, we present a description of both the physics and the associated numerical modelling strategy.

4.1. Diffusion modeling

Since the in-plane dimensions of the laminate are much larger than its thickness, it is considered that water diffusion mainly occurs in the through-thickness direction. The experimental results from section 3.1 show that the moisture uptake kinetics can be approached by a Fickian law. The water diffusion problem can therefore be treated using a 1D formulation of Fick's law, which is commonly applied in the literature [18,19].

$$\begin{cases} \dfrac{\partial C(z,t)}{\partial t} = \nabla_z D_{zz} \nabla_z C(z,t), \text{ for } -h < z < h \\ C(-h,t) = C(h,t) = C_{imp} \\ C(z,0) = C_0 \end{cases}, \qquad \text{(Equation. 4)}$$

where C is the moisture content field, t is the time, z is the through-thickness coordinate, ∇_z is the spatial differential operator along the z direction, D is the moisture diffusion coefficient in the through-thickness direction, h is the half thickness of the laminate, C_0 and C_{imp} are the initial and imposed moisture contents, respectively. For the different problems to be solved, we assume that $C_{imp} = C_s$. This problem (Eq. 4) is solved by the finite difference scheme given in *Matlab 2016a*. In this way, the mean water content value is estimated along with its distribution through the thickness of the composite.

4.2. Hygro-mechanical behaviour modelling

Due to the small thickness of the unidirectional and the asymmetric laminate compared to the dimensions along the in-plane directions, we use the modified Classical Laminate Theory proposed by

Hyer [32]. This theory is based on a postulate of the displacement field to reproduce the experimentally observed out-of-plane component *w*, which can be expressed as follows:

$$w = \frac{1}{2}\left(ax^2 + by^2\right), \qquad \text{(Equation. 5)}$$

where *x* and *y* are the in-plane general coordinates of the laminate, *a* and *b* are the curvatures of the laminate along the *x* and *y* directions, respectively. From the displacement field, and according to the Kirchhoff hypotheses, the in-plane strain components are determined with non-linear strain-displacement relationships, following the von Karman approximation of Green's strain measure:

$$\varepsilon_{xx} = \frac{\partial u^0}{\partial x} + \frac{1}{2}\left(\frac{\partial w}{\partial x}\right)^2 - z\frac{\partial^2 w}{\partial x^2},$$

$$\varepsilon_{yy} = \frac{\partial v^0}{\partial y} + \frac{1}{2}\left(\frac{\partial w}{\partial y}\right)^2 - z\frac{\partial^2 w}{\partial y^2},$$

$$\varepsilon_{xy} = \frac{1}{2}\left[\frac{\partial u^0}{\partial y} + \frac{\partial v^0}{\partial x} + \left(\frac{\partial w}{\partial x}\right)\left(\frac{\partial w}{\partial y}\right)\right] - z\frac{\partial^2 w}{\partial x \partial y},$$

where ε_{ij} are the in-plane components of the strain tensor and u^0 and v^0 are the mid-plane displacements along the *x* and *y* directions, respectively. Due to the small thickness of the laminate, the stress state is assumed to follow the plane-stress formulation. The linear hygro-elastic stress vs. strain relation can therefore be written as follows:

$$\begin{Bmatrix}\sigma_{xx}\\ \sigma_{yy}\\ \sigma_{xy}\end{Bmatrix} = \begin{bmatrix}\bar{Q}_{11} & \bar{Q}_{12} & \bar{Q}_{16}\\ \bar{Q}_{12} & \bar{Q}_{22} & \bar{Q}_{26}\\ \bar{Q}_{16} & \bar{Q}_{26} & \bar{Q}_{66}\end{bmatrix}\left(\begin{Bmatrix}\varepsilon_{xx}\\ \varepsilon_{yy}\\ \varepsilon_{xy}\end{Bmatrix} - \begin{Bmatrix}\beta_1\\ \beta_2\\ \beta_6\end{Bmatrix}\Delta C_{mean}\right), \qquad \text{(Equation. 6)}$$

where σ_{ij} are the components of the stress tensor, $\overline{Q_{ij}}$ are the components of the reduced stiffness matrix of the material expressed in the global coordinates of the laminate [33] which are obtained from the measured material parameters E_L, E_T, v_{LT} and G_{LT} according to the classical lamination theory. β_i are the coefficients of moisture expansion and ΔC_{mean} is the difference between the current and the initial moisture contents. The current moisture content corresponds to the mean value over the finite

difference nodes associated with each ply. To increase the accuracy of the model, each ply is potentially divided into several sub-plies of the same behaviour to capture the evolution of stresses through the thickness of the laminate. More details concerning this discretization can be found in [19]

Then, the total potential energy *W* of the laminate can be expressed as follows:

$$W = \frac{1}{2}\int_V \sigma_{ij}\varepsilon_{ij} dV \,, \qquad \text{(Equation. 7)}$$

where *V* is the total volume of the laminate. The computation of the W value is discussed further below.

Determination of the minimum total potential energy *W* consists of finding values for the kinematic parameters (*i.e.* the curvatures *a* and *b*, and the other parameters) so that the first variation of *W* is zero. The minimization of *W* can lead to different solutions, each corresponding to an equilibrium shape. The process of finding a solution is thus completed by applying a stability criterion, which consists of calculating the second derivative of *W*. If this latter is positive, the solution is stable and *vice versa*. The whole resolution procedure is performed within the *Symbolic Math* toolbox in *Matlab 2016a*. For more details on the resolution procedure and the stability criterion, the reader should refer to [32]. Once the different values of *a*, *b* and the other parameters are determined for a given moisture content, it is possible to estimate the stress and strain distributions through the thickness of the laminate. This distribution can be given either in the global laminate coordinates (*x,y,z*) or in the local coordinate system of each independent ply (*1,2,3*). In the case of a unidirectional ply, the direction 1 corresponds to the longitudinal direction of the fibres, and 2 to the in-plane transverse direction.

This approach has already been adapted to the study of hygroscopic stress development in asymmetric composite laminates [34,35]. However, this approach concerns the study of glass or carbon fibres in epoxy matrix composites, and does not take into account plasticization of the material during moisture diffusion.

5. Numerical results

The composite behaviour is numerically reproduced from the material properties identified in section 3 and the model developed in section 4. First, we discuss the diffusion modelling used for both ply

sequences. Then, we focus on the hygromechanical behaviour of the UD laminate. Finally, we investigate the hygromechanical response of the asymmetric laminate through its curvature and stress distribution through the laminate thickness.

5.1 Diffusion modeling

The properties identified in section 3.1 are used as direct input into the diffusion model described in section 4.1. The thicknesses of the unidirectional and the asymmetric laminates are set at 0.46 mm. The spatial and temporal convergence is checked for both numerical simulations, leading to 200 finite difference nodes and a time step of 20 s which ensures accuracy of the results.

Figure 6 shows the variation of mean moisture content C_{mean} (computed from the finite difference scheme for both the UD and the bilaminar ply sequences) compared with the experimental values determined in section 3.1. Once again, we find an excellent agreement, which thus reveals the ability of the hygroscopic model to describe the material behaviour.

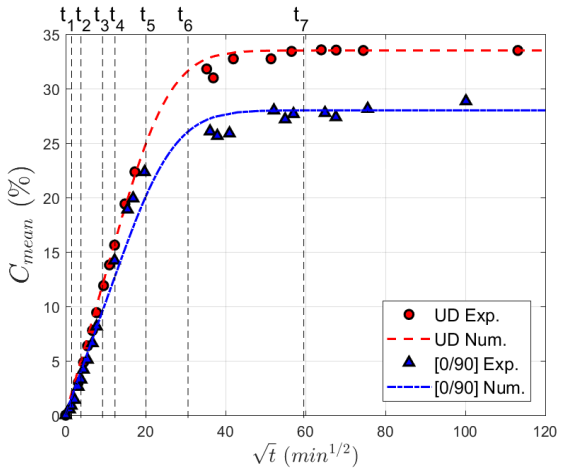

Figure 6: Evolution of the experimental and modelled mean moisture content for both ply sequences. Error bars on the experimental results are not represented for the sake of clarity but can be found in Fig. 1.

Figure 6 also shows the characteristic diffusion time t_i, with i varying from 1 to 7. For each t_i, it is possible to calculate the moisture content distribution through the laminate thickness (Fig 7). The distribution of moisture across the thickness highlights the heterogeneous distribution of moisture from the edge (Z = ± 0,24) to the centre (z=0) of both samples during the diffusion process (t_1 to t_7).

As increasing moisture leads to a drastic effect on the hygro-mechanical properties of biocomposites, the moisture distribution also involves a variation of this effect throughout the laminates.

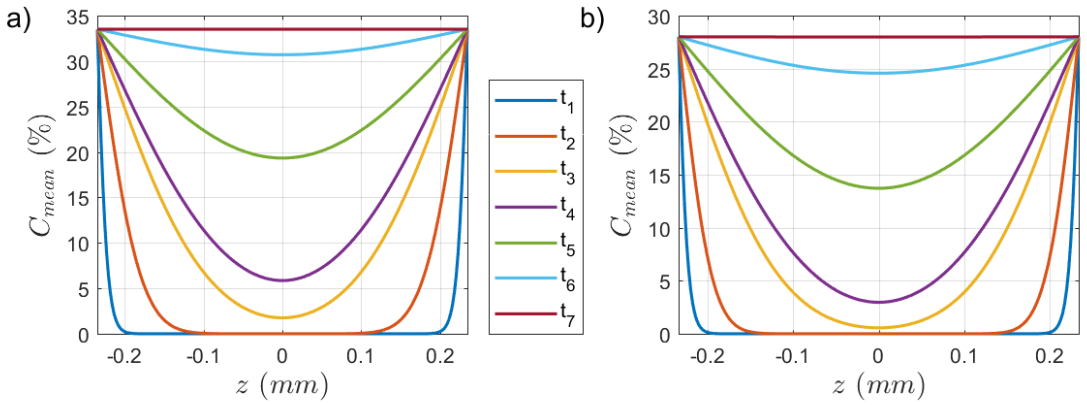

Figure. 7: Moisture distribution across the thickness of unidirectional (a) and asymmetric lay up (b) for different diffusion times t_i.

5.2 Hygroscopic swelling of the unidirectional laminate

From the model developed here, it is possible to estimate the in-plane strain for the unidirectional biocomposites during the diffusion process. Numerical results plotted as a function of the mean moisture content $C_{mean\ UD}$ are compared to experimental results and highlight a good correlation (Fig. 8). Hygroscopic strains vary non-linearly with moisture contents of up to 15% due to the evolution of mechanical properties (see Fig 3). At higher moisture content, a linear trend is predicted by the model. The largest difference (18%) between the experimental and numerical data occurs for a mean content of C_{mean} = 22.5%, which corresponds to a hygroscopic strain of 2.84 ± 0.11 %.

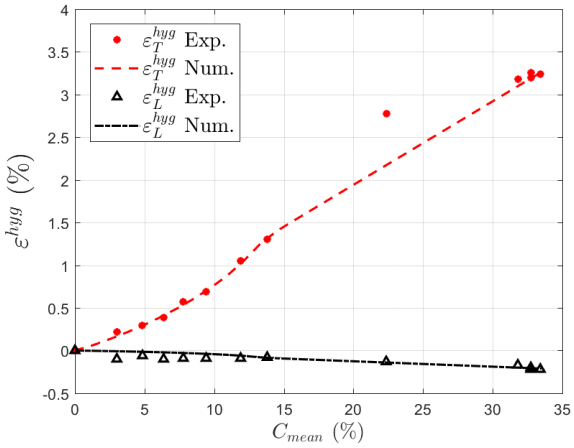

Figure 8: Experimental and predicted evolution of longitudinal and transverse strain in the unidirectional laminate.

From the numerical modeling, we can obtain the stress distribution within the material thickness. This allows us to lay specific emphasis on the potential coupling between stress state and moisture diffusion. For a MAPP/flax unidirectional laminate, the transverse stress σ_{22}n corresponds to the transverse direction with respect to the fibres. This parameter is specifically investigated here since it illustrates a case of severe loading for the material used to target the fibre/matrix interface properties. Evolution of the transverse stress σ_{22} and moisture-induced damage should influence the moisture diffusion behaviour of composites [36]. Figure 9 shows the distribution of σ_{22} for different characteristic times t_i.

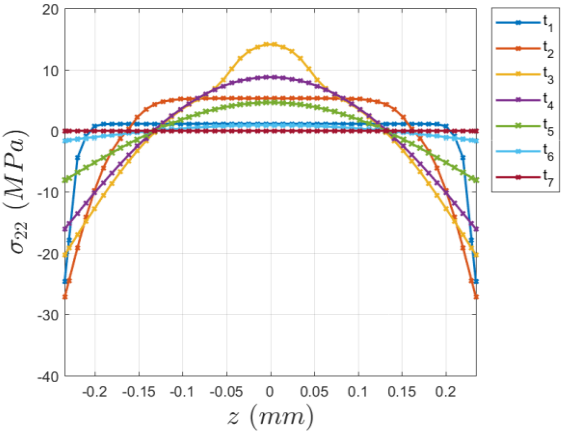

Figure 9: Distribution through the material thickness of the transverse component of the stress tensor σ_{22}, for different characteristics times t_i.

During the moisture diffusion process, the plies located in the external part of the section are the first to undergo moisture diffusion and hygroscopic swelling. However, these external plies suffer from neighboring constraints from internal plies due to differential swelling [22][37]. The latter have a lower moisture content and therefore a lower swelling strain. Hence, the external plies are in a compression state and, conversely, plies located towards the centre undergo tensile stresses. This stress state can be determined for each characteristic time, and the maximum values for tensile or compression are found at t_2 and t_3. This corresponds to the time when the moisture diffusion reaches the centre of the material (Fig 7a). At this sorption time, the material at the centre is still dry and subject to a tensile stress of around 15 MPa, which is double compared to the transverse tensile strength measured at the dry state (Fig 3). When saturation is reached (t_7 on Figure 6), there is no longer any moisture gradient in the material thickness, so the resulting stress state is consequently nil. This is however to be considered with care as the developed model only described the behavior of homogeneous equivalent plies. At the fibers scale, the matrix do not swells compared with the fiber leading to a compressive state around the fiber along their radial direction. These phenomenon are however not considered in the present study.

5.3 Hygro-mechanical behaviour of the asymmetric laminate

5.3.1 Curvature

Because of the swelling of each ply composing the asymmetric laminate, this latter exhibits a curvature due to the difference in behaviour between plies oriented at 0° and plies oriented at 90°. This curvature is experimentally measured (as described in section 2.2.4) and numerically predicted by the model developed here. At saturation, the experimentally measured curvature reaches 0.08 mm^{-1}, whereas the model predicts a value of the curvature a = 0.087 mm^{-1}, and of the curvature b = 0.003 mm^{-1} which is considered negligible. This represents an error of 8.7% with the measured curvature along the x direction, which reflects the ability of the model to reproduce the effective behaviour of the bilaminar material.

5.3.2 Hygroscopic stress state

The distribution of stresses through the laminate thickness is obtained using the model developed in this study. Figure 10 represents the stresses components σ_{xx} and σ_{yy} distribution through the thickness of the laminate for each specific time t_i. The delimitation between the five plies at 90° and the ply at 0° is also represented on this graph.

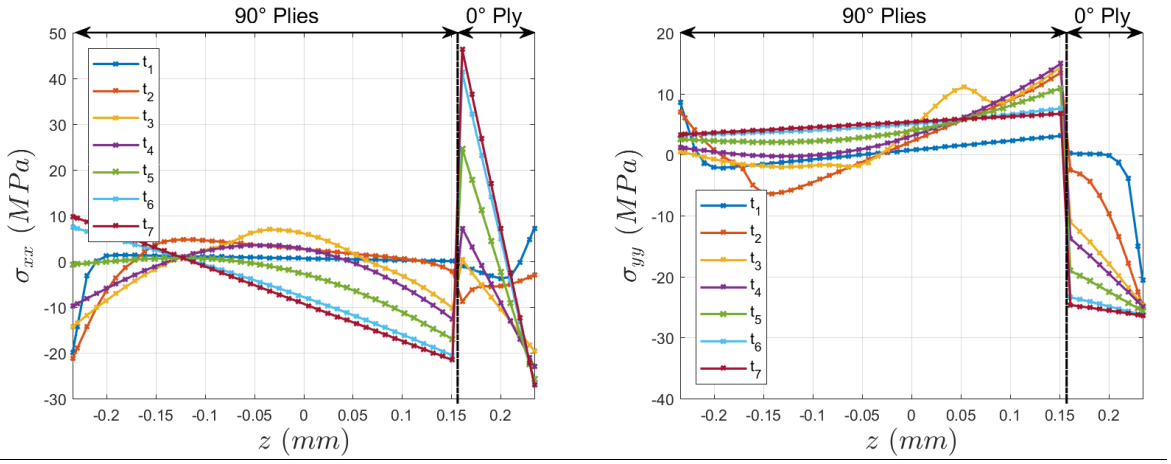

Figure 10: Distribution of the global stress components σ_{xx} and σ_{yy} through the thickness of the asymmetric laminate for different characteristic times t_i.

The stresses distribution is more complex compared to the unidirectional case. During the first time steps (at t_1 and t_2), the moisture is only present near the laminate surfaces. The external plies are therefore the first to undergo hygroscopic swelling along their transversal direction and to a small contraction along their longitudinal direction, but they are blocked by the internal ply which are still dry. This leads to a compressive stress for the external 90° and 0° plies along the x and y direction, respectively, and to a tensile stress for the external 90° and 0° plies along the y and x direction, respectively. As moisture diffuses through the thickness of the laminate, the stresses distribution then evolves to reach the distribution at the equilibrium state (t_7). The stresses distribution at this final step corresponds to that of an asymmetric composite submitted to bending as described in [33]. In the *x* direction, the outer 90° plies (from *z* = -0.234 to -0.125mm) are submitted to a tensile stress whereas the internal plies (from *z* = -0.125 to 0.156mm) are submitted to a compressive stress. The 0° ply undergoes a compressive stress at the outer surface and a tensile stress at the interface between the 0° ply and the 90° plies. This stress distribution for the *x* direction is due to the curvature *a* of the laminate. In the y direction, the 90° plies are submitted to a tensile stress and the 0° ply to a compressive stress due to the curvature *b* of the laminate.

From these stresses distribution, it is possible to extract the distribution of the stress component transverse to the fiber, *i.e.* σ_{22} in the local coordinate system of each ply. It corresponds to σ_{xx} for the 90° plies and to σ_{yy} for the 0° plies. It is represented for each specific time t_i in Figure 11.

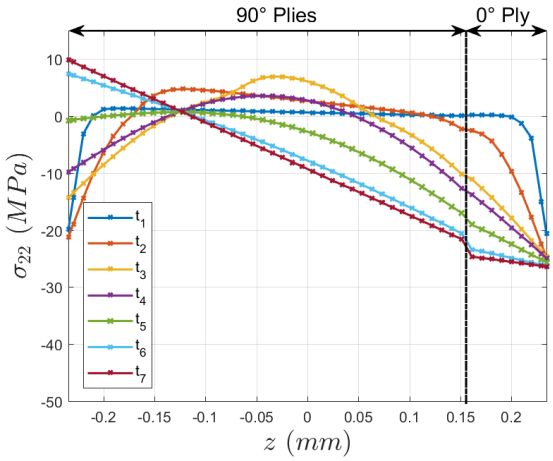

Figure 11: Distribution of the transverse stress component σ_{22} through the thickness of the asymmetric laminate for different characteristic times t_i.

The previous analysis leads to several observations concerning this stresses distribution. During the first time steps represented in Fig. 11 (from t_1 to t_4), the external plies are the first to undergo hygroscopic swelling, but they are blocked by the internal plies. This differential swelling leads to a compression stress state in peripheral plies, whereas the internal plies are subject to a tensile stress state. The stress distribution is then modified from t_4 to the end of the saturation. The ply at 0° tends to swell steadily during diffusion, but it is however blocked by the surrounding plies at 90°, which are little deformed along their longitudinal direction. The 0° ply is therefore highly constrained, and subject to a compression stress state along its transverse direction during the whole diffusion process. The plies at 90° then exhibit a stress distribution corresponding to the saturation of the laminate (t_7). The external 90° plies (from z = -0.234 to -0.125mm) are subject to a tensile stress state from t_5 to saturation, whereas the internal plies (from z = -0.125 to 0.156 mm) undergo a compression stress state from t_5 to saturation.

6. Discussion

As pointed out in section 3.1, there is a significant difference between the maximal sorption ability of unidirectional and asymmetrical MAPP/flax laminates (Figure 1). These two ply sequences were

obtained from the same material, with identical dimensions, fibre content and manufacturing process. The only relevant difference arises from the lay-up sequences. Because the two lay-up sequences induces different internal stresses during water absorption, we can assume that the hygroscopic behaviour is dependent on the stress state. Indeed, for the asymmetrical biocomposite, most of the plies remain in compression while being saturated. This leads to a reduction of free volume within the composite, which consequently reduces the moisture uptake. This phenomenon has already been observed for polymeric composites and is greatly influenced by the initial porosity [38][36].

In addition, the moisture gradient in the unidirectional laminate during diffusion, combined with the evolution of mechanical properties, leads to a tensile state within the internal plies of the laminate. The estimated transverse tensile stresses (with a maximum value of 15 MPa) are higher than the transverse strength (estimated at 2.9±0.2 MPa). Therefore, damage could occur by cracking, leading also to a potentially faster moisture uptake. This suggests that the differential swelling occurring between plies could be a degradation mechanism for natural fibre composites even with a simple unidirectional lay-up.

The curvature of experimental asymmetric laminate during moisture uptake shows a linear increase followed by stabilization for moisture contents higher than 10% (Fig. 5). However, the free swelling of the unidirectional ply continues far beyond this content until saturation (Fig. 8). Several possible explanations can be proposed from the different results of this study. First, the estimated values of transversal stress calculated from the model (with a maximum of 5 MPa in the internal 90° plies) are higher than the material strength along this direction (with a value of 2.9±0.2 MPa). Therefore, it is probable that the material undergoes damage, thus confirming previous observations on natural fibre composites [39] and asymmetric hygromorph biocomposites [17]. Moreover, flax fibres are mainly composed of polysaccharides, hemicelluloses and pectins, whose mechanical properties and glass transition temperature Tg strongly depend on the moisture uptake [40][41]. The leaching of low molar weight polysaccharides such as pectins would lead to the degradation of fibres [39] and fibre/matrix interfaces due to void formation [42]. This damage can then modify the sorption behaviour of the material, creating more free volume.

4. Conclusion

This study experimentally investigates the moisture uptake in a bio-sourced composite (composed of compatibilized polypropylene with grafted maleic anhydride and reinforced with 60%$_{Vol}$ of flax fibres) with several ply sequences. The two studied ply sequences correspond to a unidirectional and an asymmetric composite, with ply sequences of [90_6] and [0_1, 90_5], respectively. This study points out that diffusion kinetics is highly impacted by the ply-sequence. As the materials used and initial dimensions are the same for both ply sequences, this modification of properties could be explained by the different strain and stress states between unidirectional and asymmetric laminates. From the model developed here, we can predict the curvature induced after moisture diffusion in the asymmetric laminate, together with the associated stress state. The final curvature values fall in a narrow range with only 8.7% difference with the experimental results. The stress state determined through the thickness of the asymmetric lay-up demonstrates that most of the plies (approx. 75% of the whole laminate) are subject to a compressive stress state along their in-plane direction transverse to the fibres. This stress distribution may lead to a decrease in the free-volume of the material, thus altering its hygroscopic properties by reducing the maximum moisture content compared to the unidirectional laminate (the stress distribution being nil for this latter when saturation is reached).

5. References

[1] Hill CAS, Norton A, Newman G. The Water Vapor Sorption Behavior of Natural Fibers. J Appl Polym Sci 2009;112.

[2] le Duigou A, Merotte J, Bourmaud A, Davies P, Belhouli K, Baley C. Hygroscopic expansion: A key point to describe natural fibre/polymer matrix interface bond strength. Compos Sci Technol 2017;151. doi:10.1016/j.compscitech.2017.08.028.

[3] A Le Duigou, S Requile, J Beaugrand, F Scarpa, M Castro,. Natural fibres actuators for smart bio-inspired hygromorph biocomposites. Smart Mater Struct 2017;26.

[4] Cichocki Jr. F. Thermoelastic anisotropy of a natural fiber. Compos Sci Technol 2002;62:669–78. doi:10.1016/S0266-3538(02)00011-8.

[5] Le Duigou A, Castro M. Evaluation of force generation mechanisms in natural, passive hydraulic actuators. Sci Rep 2016;18105.

[6] Almgren KM, Gamstedt EK. Characterization of Interfacial Stress Transfer Ability by Dynamic Mechanical Analysis of Cellulose Fiber Based Composite Materials. Compos Interfaces 2010;17:845–61. doi:10.1163/092764410X539235.

[7] Sar BE, Fréour S, Davies P, Jacquemin F. Coupling moisture diffusion and internal mechanical states in polymers – A thermodynamical approach. Eur J Mech - A/Solids 2012;36:38–43. doi:10.1016/j.euromechsol.2012.02.009.

[8] Joffre T, Wernersson ELG, Miettinen A, Luengo Hendriks CL, Gamstedt EK. Swelling of cellulose fibres in composite materials: Constraint effects of the surrounding matrix. Compos Sci Technol 2013;74:52–9. doi:10.1016/j.compscitech.2012.10.006.

[9] A. Célino, S. Fréour, F.Jacquemin, P. Casari. The hygroscopic behavior of plant fibers: a review. Front Chem 2014;1:1–12.
[10] Faruk O, Bledzki AK, Fink H-P, Sain M. Biocomposites reinforced with natural fibers: 2000–2010. Prog Polym Sci 2012;37:1552–96. doi:10.1016/j.progpolymsci.2012.04.003.
[11] Azwa ZN, Yousif BF, Manalo AC, Karunasena W. A review on the degradability of polymeric composites based on natural fibres. Mater Des 2013;47:424–42. doi:http://dx.doi.org/10.1016/j.matdes.2012.11.025.
[12] Parlevliet P, Bersee H and BA. Residual stresses in thermoplastic composites--A study of the literature--Part I: Formation of residual stresses. Comp Part A Appl Sci Manuf 2006;37:1847–57.
[13] M. Gigliotti, M.R. Wisnom KDP. Development of curvature during the cure of AS4/8552 [0/90] unsymmetric composite plates. Compos Sci Technol 2003;63:187–97.
[14] Gigliotti M, Molimard J, Jacquemin F, Vautrin A. On the nonlinear deformations of thin unsymmetric 0/90 composite plates under hygrothermal loads. Compos Part A Appl Sci Manuf 2006;37:624–9. doi:10.1016/j.compositesa.2005.05.003.
[15] Le Duigou A, Castro M, Bevan R, Martin N. 3D printing of wood fibre biocomposites: From mechanical to actuation functionality. Mater Des 2016;96:106–14. doi:10.1016/j.matdes.2016.02.018.
[16] Le Duigou A, Castro M. Moisture-induced self-shaping flax-reinforced polypropylene biocomposite actuator. Ind Crops Prod 2015;71. doi:10.1016/j.indcrop.2015.03.077.
[17] Le Duigou A, Castro M. Hygromorph BioComposites: Effect of fibre content and interfacial strength on the actuation performances. Ind Crops Prod 2017;99. doi:10.1016/j.indcrop.2017.02.004.
[18] Lee MC, Peppas NA. Models of moisture transport and moisture induced stresses in epoxy composites. J Compos Mater 1993;27:1146–71.
[19] Benkeddad A, Grédiac M, Vautrin A. On the transient hygroscopic stresses in laminated composite plates. Compos Struct 1995;30:201–15.
[20] Vaddadi P, Nakamura T, Singh RP. Transient hygrothermal stresses in fiber reinforced composites: a heterogeneous characterization approach. Compos Part A Appl Sci Manuf 2003;34:719–30.
[21] Mercier J, Bunsell A, Castaing P, Renard J. Characterization and modeling of aging of composites. Compos Part A Appl Sci Manuf 2008;39:428–38.
[22] Youssef G, Fréour S, Jacquemin F. Stress-dependent moisture diffusion in composite materials. J Compos Mater 2009;43:1621–37.
[23] Jain D, Mukherjee A, Kwatra N. Effect of fibre topology on hygro-mechanical response of polymer matrix composites. Int J Heat Mass Transf 2015;86:787–95.
[24] Obeid H, Clément A, Fréour S, Jacquemin F, Casari P. On the identification of the coefficient of moisture expansion of polyamide-6: Accounting for differential swelling strains and plasticization. Mech Mater 2018;118:1–10.
[25] Regazzi A, Léger R, Corn S, Ienny P. Modeling of hydrothermal aging of short flax fiber reinforced composites. Compos Part A Appl Sci Manuf 2016;90:559–66.
[26] Le Duigou A, Davies P, Baley C. Seawater ageing of flax/poly(lactic acid) biocomposites. Polym Degrad Stab 2009;94:1151–62. doi:10.1016/j.polymdegradstab.2009.03.025.
[27] Alben S, Balakrisnan B, Smela E. Edge Effects Determine the Direction of Bilayer Bending. Nanoletter 2011;dx.doi.org.
[28] DU. Shah, PJ. Schubel, MJ. Clifford PL. The Tensile Behavior of Off-Axis Loaded Plant Fiber Composites: An Insight on the Nonlinear Stress–Strain Response. Pollymer Compos 2012;1454-1504.
[29] J. Crank. The mathematics of diffusion. Clarendon Press Oxford, 1975.
[30] Assarar M, Scida S, Mahi E, Poilâne C, Ayad R. Influence of water ageing on mechanical properties and damage events of two reinforced composite materials: Flax–fibres and glass–fibres. Mater Des 2011;32.
[31] A Le Duigou, V Keryvin, J Beaugrand, M Pernes, F Scarpa MC. Humidity responsive actuation of bioinspired Hygromorph BioComposites (HBC) for adaptive structures. Comp Part A Appl Sci Manuf 2018.

[32] Hyer M. Calculation of the room-temperature shapes of unsymmetric laminates. J Compos Mater 1981;15:296–310.
[33] Herakovich CT. Mechanics of fibrous composites. John Wiley & Sons; 1998.
[34] Gigliotti M, Jacquemin F, Molimard J, Vautrin A. Transient and cyclical hygrothermoelastic stress in laminated composite plates: Modeling and experimental assessment. Mech Mater 2007;39:729–45.
[35] Telford R, Katman KB, Young TM. The effect of moisture ingress on through-thickness residual stresses in unsymmetric composite laminates: A combined experimental-numerical analysis. Compos Struct 2014;107:502–11.
[36] Humeau C, Davies P, F Jacquemin, Humeau C, Davies P FJ. Moisture diffusion under hydrostatic pressure in composites. Mater Des 2016;96:90–8.
[37] MJ Adamson. Thermal expansion and swelling of cured epoxy resin usezd in graphite/epoxy composite materials. J Mater Sci 1980;15:1736–45.
[38] Autran, M., Pauliard, R., Gautier, L., Mortaigne , B., Mazeas, F., Davies, P. Influence of mechanical stresses on the hydrolytic aging of standard and low styrene unsaturated polyester composites. J Appl Polym Sci 2002;84:2185–95.
[39] Le Duigou A, Bourmaud A, Baley C. In-situ evaluation of flax fibre degradation during water ageing. Ind Crops Prod 2015;70:204–10. doi:10.1016/j.indcrop.2015.03.049.
[40] Cousins WJ. Young's modulus of hemicellulose as related to moisture content. Wood Sci Technol 1978;12:161–7.
[41] Basu, S., Shivhare, U. S., & Muley S. Moisture adsorption isotherms and glass transition temperature of pectin. J Food Sci Technol 2013;50:585–9.
[42] Le Duigou A, Davies P, Baley C. Exploring durability of interfaces in flax fibre/epoxy micro-composites. Compos Part A Appl Sci Manuf 2013;48:121–8. doi:10.1016/j.compositesa.2013.01.010.